J Acupunct Meridian Stud 2010;3(2):81–88

RESEARCH ARTICLE

ELSEVIER

Primo-Vessels as New Flow Paths for Intratesticular Injected Dye in Rats

Hyun-Jung Han[1], Vyacheslav Ogay[1], Sang-Jun Park[1,2], Byung-Cheon Lee[1,2], Ki-Woo Kim[3], Yu Won Lee[4], Jin-Kyu Lee[4], Kwang-Sup Soh[1]*

[1]*Biomedical Physics Laboratory, Department of Physics and Astronomy and Center for Theoretical Physics, Seoul National University, Seoul, Korea*
[2]*Korean Pharmacopuncture Institute, Seoul, Korea*
[3]*National Instrumentation Center for Environmental Management, College of Agriculture and Life Sciences, Seoul National University, Seoul, Korea*
[4]*Materials Chemistry Laboratory, School of Chemistry, Seoul National University, Seoul, Korea*

Received: Feb 4, 2010
Accepted: Apr 14, 2010

KEY WORDS:
chromium hematoxylin;
nanoparticle;
novel flow path;
primo-vessels;
testis

Abstract
After intratesticular injection of a chromium hematoxylin and fluorescent nanoparticle solution, we found a novel flow path in the abdominal cavity consisting of primo-vessels and primo-nodes. This flow path formed a network that crossed over the surfaces of abdominal organs, and generally linked to the greater omentum and adjacent visceral peritoneum. Some of these structures terminated at organs such as the small intestine and the urinary bladder; occasionally, the network entered the parenchyma of organs. The semitransparent primo-vessels and nodes were wholly or partially stained dark-blue by chromium hematoxylin. Injected nanoparticles were also observed in primo-vessels and nodes as well as the parenchyma of organs which were the site of primo-vessel termination. Transmission electron microscopy showed that the primo-vessels consist of many sinuses (4–6 μm), surrounded by collagen fibers, specific granules, cellular remnants, immune cells, extracellular matrices, and hematopoietic cells. These histological features are completely different from blood and lymph vessels indicating that primo-vessels are novel structures that allow the flow of dye.

1. Introduction

Testes have three main circulatory paths including sperm-transfer, blood circulation and the lymphatic drainage. Previous reports investigating the circulation of the testes using intratesticular injection of various dyes demonstrated that most dyes passed into the systemic circulation through the blood and lymphatic vessels and were filtered into the urine [1–3]. The injected dye could not flow through the path for sperm-transfer because it did not pass into the seminiferous tubules [4]. In the case of long-term observation, some of the injection dyes remained on the testes and were taken up by macrophages after 24 hours [4].

As far as we are aware, no other flow paths after intratesticular injection have been reported. Here, we report our finding of a novel flow path consisting of primo-vessels (PVs). PVs have already been reported and named novel threadlike-structures or

*Corresponding author. Biomedical Physics Laboratory, Department of Physics and Astronomy and Center for Theoretical Physics, Seoul National University, Gwanak 599 Gwanak-ro, Gwanak-gu, Seoul 151-747, Korea.
E-mail: kssoh1@gmail.com

Bonghan ducts in previous studies [5–9]. They were, in fact, discovered by Bong-Han Kim about 40 years ago [10], and this finding was partially confirmed by Fujiwara and Yu [11]. An intensive re-investigation has been performed by the research team in Seoul National University in Korea, with funding provided by the National Research Laboratory program of the Korean Ministry of Science and Technology. As a result, many characteristics of the novel structure have been confirmed by introducing new methods and employing modern techniques. PVs are thin, threadlike, semitransparent and vascularized. Oval or cucumber-like nodes are located irregularly along a PV. PVs were found inside blood vessels [5,12–16], lymphatic vessels [7,17–20], in the brain, the spinal cord [21], and on the surfaces of internal organs [6,22,23], connecting with each other to form a network. The flow inside PVs has been studied. Magnetic nanoparticles flowed in PVs after intra-node injection [24], and Alcian blue dye also flowed in PVs on the surface of an abdominal organ [8]. Furthermore, the flow speed of dye has been confirmed as slow at 0.3 ± 0.1 mm/s [8].

The present study was designed based on the observation that PVs form a network for flow throughout the body. To demonstrate whether there is some flow through PVs, a solution of chromium hematoxylin (Cr-Hx) mixed with fluorescent nanoparticles was injected into the testicular parenchyma, and the stained PVs were observed and analyzed using confocal laser scanning microscopy (CLSM), immunohistochemical techniques, and transmission electron microscopy (TEM).

2. Materials and Methods

2.1. Animal preparation

Fifteen male Sprague Dawley rats were used in this study. They ranged from 9–12 weeks in age and from 150–250 g in weight. The animals were housed in a temperature-controlled environment (23°C) with 60% relative humidity and a 12 hour light/dark cycle. They had *ad libitum* access to food and water. The procedures involving the animals and their care were in full compliance with current international laws and policies [25]. The study design and experimental protocols were approved by the Institute of Laboratory Animal Resources of Seoul National University.

2.2. Injection of Testes with Cr-Hx and fluorescent nanoparticle solution

Filtered Cr-Hx mixed with a solution of fluorescent nanoparticles was prepared to visualize threadlike structures and to trace the circulatory paths of the PVs. The Cr-Hx solution was made by mixing 3% chromium potassium solution and 1% hematoxylin solution. Next, potassium iodate (0.1 g) was added to the mixed solution. The solution was then boiled until blue, and cooled to room temperature.

The fluorescent nanoparticles solution was made following procedures described in previous studies [7,26] and employing a modified polyvinylpyrrolidone method. This resulted in the formation of cobalt–ferrite magnetic nanoparticles coated with a shell of amorphous silica [7,26]. A luminescent organic dye, rhodamine B isothiocyanate [orange, λmax(em) = 555 nm], was present inside the silica shell and biocompatible poly(ethylene glycol) was present on the outside. The average size of the water-soluble bare cobalt–ferrite magnetic nanoparticles was approximately 9 nm. The total size of the core-shell structure was approximately 50 nm. The concentration of nanoparticles was 2.0 mg/cm^3, and they were suspended in a sterile saline solution at pH 7.4.

The Cr-Hx and fluorescent nanoparticle solution was mixed at a 1:1 ratio, and the total injection volume was 200 μL (100 μL:100 μL) in each testis. Under general anesthesia (xylazine, 10 mg/kg, plus ketamine, 70mg/kg, intramuscular injection), the mixed solution was slowly injected into the testicular parenchyma by using a 26-guage needle attached to a 1 mL plastic disposable syringe. The dye was injected into three points equally located on the lateral sides of the scrotum and there was no backflow.

2.3. Stereomicroscope and fluorescence reflectance imaging

At 24 hours after the injection, the rats were euthanized using ether, and the abdominal cavity and the testes were observed to detect Cr-Hx-stained PVs. These observations were performed under a stereomicroscope (SZX12; Olympus, Tokyo, Japan), and images were captured using a digital camera (Nikon, Tokyo, Japan). After taking the sample to detect fluorescent nanoparticles, true-color fluorescence imaging was accomplished by using a specific illumination system. Fluorescence emission from the nanoparticles was detected with a stereomicroscope, a sensitive color charged-coupled device (CCD) camera (DP 70; Olympus) using a long-pass filter (600 nm; CVI, Seoul, Korea), and a fluorescence microscope (MVX10; Olympus).

2.4. Whole-mounted staining

For whole mounted preparations, tissue specimens were fixed overnight in 4% paraformaldehyde in phosphate buffered saline and were then pretreated

with 3% sodium deoxylate solution for 4 hours at room temperature. The specimens were blocked overnight at 4ºC in 10% fetal bovine serum prior to incubation overnight with rat anti-mouse CD31 (1:50; BD Pharmingen, San Jose, CA, USA). After washing in phosphate buffered saline, the specimens were stained with Alexa Fluor 488 conjugated goat anti-rat antibody IgG (H+L; 1:500; Invitrogen, Eugene, OR, USA). Whole mount specimens were stained by using 4′,6-diamidino-2-phenylindole, or DAPI (a specific dye for DNA), mounted in anti-fading medium, and observed with a multi-photon CLSM (LSM 510-NLO; Carl Zeiss, Göttingen, Germany).

2.5. TEM

For TEM, tissues were fixed with 2.5% glutaraldehyde in a 0.1 M sodium cacodylate buffer (pH 7.2) overnight at 4ºC. The specimens were postfixed in 1% OsO_4 in a 0.2 M sodium cacodylate buffer for 1 hour, dehydrated with ethanol and propylene oxide, and embedded in epoxy resin (Epon 812). Semi-thin and ultra-thin sections were obtained using an ultramicrotome LKB 4802 system. The semi-thin sections were stained with 1% toluidine blue (dissolved in 1% borax) and photographed using a light microscope (BX51, Olympus) to study gross morphology. The ultra-thin sections were collected on large-scale copper grids, contrasted by using 2% uranyl acetate and Reynolds' lead citrate, and then examined in a TEM (JEM 1010; JEOL, Tokyo, Japan) at an accelerating voltage of 80 kV. Images were obtained by using a digital camera (ES1000W; Gatan Inc., Pleasanton, CA, USA) and were processed with software (Gatan Inc.).

2.6. Image analysis

Confocal images were analyzed using Image Browser 5 LSM, v3.5 (Carl Zeiss), by performing orthogonal sectioning, a three-dimensional projection analysis, and morphometric examination.

3. Results

Of the 15 rats, 10 rats displayed PVs which were stained by Cr-Hx and nanoparticles in the abdominal cavity (Table 1). The PVs were floating over the surfaces of abdominal organs, including the liver, spleen, duodenum, jejunoileum, cecum, colon, urinary bladder and prostate gland (Figure 1). The PVs started from the lower region of the abdomen, such as the urinary bladder, prostate gland, ductus deferens, and fat tissue surrounding the testes, to the upper region of the abdomen, including the greater omentum, liver and abdominal wall. The structures were connected to each other and formed a network.

The structures were thin, semitransparent, and flexible, with a diameter around 50 μm. The cucumber shaped nodes, around 500 μm × 200 μm in size, were linked by PVs at both their ends (Figures 1B, 1D, and 1F). The node was also semitransparent, and some of contained blood (Figure 1F). These

Table 1 Overall data on primo-vessels (PVs) in rat abdominal cavity after 24 hours of intratesticular injection of chromium hematoxylin and fluorescent nanoparticles

Sprague Dawley rat			Presence of PVs*	Region of PV distribution
No.	Age (wk)	BW (g)		
1	9	169	Yes	Urinary bladder–intestine–liver–right abdominal wall
2	10	178	Yes	Ductus deferens–intestine–great omentum–right abdominal wall
3	10	183	No	–
4	10	210	No	–
5	9	192	Yes	Prostate gland–intestine–liver
6	10	205	Yes	Intestine–great omentum–right abdominal wall
7	10	223	Yes	Urinary bladder–spleen–great omentum–liver–left abdominal wall
8	12	248	Yes	Right abdominal wall–great omentum–liver
9	11	221	No	–
10	10	225	Yes	Jejunoileum–intestine–spleen–great omentum
11	10	201	Yes	Urinary bladder–spleen
12	9	175	Yes	Intestine
13	11	230	Yes	Right abdominal wall–intestine–spleen
14	11	234	No	–
15	10	220	No	–

*PVs were partially or wholly stained by chromium hematoxylin under the stereomicroscope. BW=body weight.

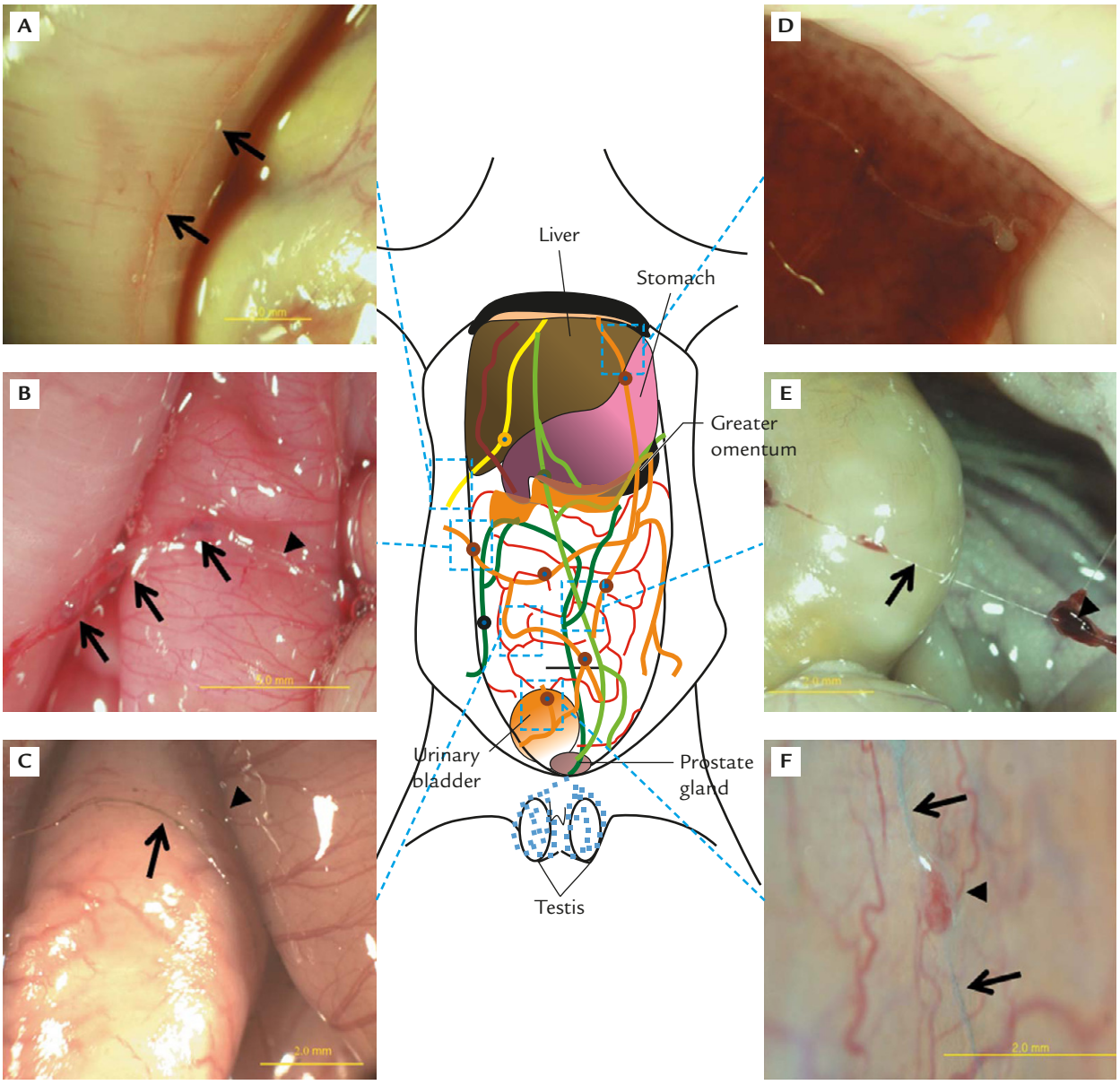

Figure 1 Primo-vessels (PVs) and nodes forming a network on the surface of an abdominal organ. (A) Semitransparent PV located on the right upper abdominal wall (arrows). (B) Three nodes stained by chromium hematoxylin (Cr-Hx) were located from the abdominal wall to the small intestine (arrows). These were connected by semi-transparent PVs, and the structures continued to adjacent intestine and connective tissue (arrowhead). (C) Cr-Hx stained PV floating on the small intestine (arrow). This PV branched out to thinner structures stained by Cr-Hx (arrowhead). (D) Cr-Hx stained PV and a node floating on the liver. (E) Semitransparent PVs (arrow) floating on the colon, with a branch point (arrowhead). A blood clot was attached to the PV. (F) PV and a node on the surface of the urinary bladder. Some blood was centrally located in the node (arrowhead) with no blood vessels in the PV (arrows).

structures were partially or wholly stained by Cr-Hx that flowed within the structures.

Some of the PVs entered the parenchyma of several organs, including the jejunoileum (Figure 2) and the urinary bladder. The immunohistochemistry of the entry point of the PVs into the jejunoileum showed fluorescent nanoparticles flowing through the PV inside the organ-parenchyma (Figure 2).

To investigate the ultra-structure and to reveal the localization of injected fluorescent nanoparticles in the PVs, we performed electron microscopic examinations (Figure 3). Figure 3A shows a semi-thin cross section of the PV found on the surface of the abdominal muscle wall. The PV measured about 40 μm in diameter and has several cavities in cross-sectional images. It attached to the muscle fiber and surrounded connective tissues. In TEM, the PV was cribriform with numerous sinuses. The diameters of the sinuses varied from 2 to 6 μm (Figures 3B and 3C). The sinuses were surrounded by collagenous

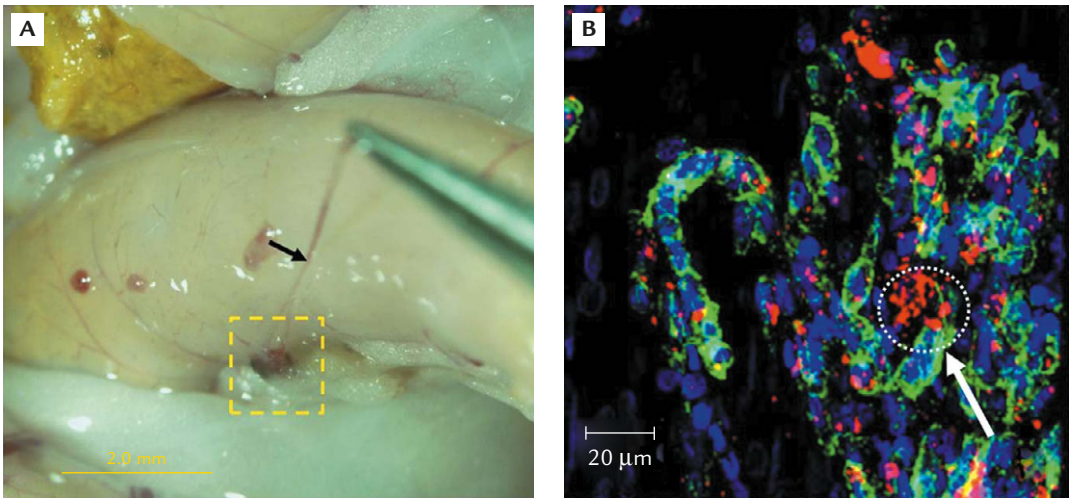

Figure 2 A primo-vessel enters an abdominal organ. (A) A primo-vessel (black arrow) is attached to the small intestine adjacent the mesentery. (B) Cross section of the rectangular area of (A) was analyzed by immunohistochemistry. It shows that red fluorescent nanoparticles (white arrow) flow into the muscularis externa of the intestine through the PV.

fibers and some sinuses contained cytoplasmic granules and cellular remnants (Figure 3C).The fluorescent nanoparticles were observed in the PVs and most of them were engulfed by phagocytes such as macrophages and neutrophils present just outside the sinuses (Figures 3D and 3E). Moreover, in distinct sites of the PV, small clusters of mature erythrocytes and their precursors, early reticulocytes, were observed (Figure 4). Like mature red blood cells (RBCs), reticulocytes did not have a cell nucleus. The cytoplasm of the reticulocytes contained mitochondria, ferritin granules, pinocytotic vesicles, and vacuoles whereas the cytoplasm of erythrocytes was entirely filled with hemoglobin and did not contain typical organelles and cytomembranes.

4. Discussion

Until now, lymph nodes were the only structure stained by dye following intratesticular injection, giving evidence for lymphatic flow of the dye [3]. However, in this study, we found a novel threadlike structure stained by injected dye, PVs, providing evidence for a novel flow path for the dye.

The gross and histological features of the PVs in this study agree with previously reported characteristics of PVs [5,6,8,27]. Furthermore, PVs were totally different from established structures such as blood and lymphatic vessels, which were generally known as flow paths for intratesticular injected dye and nerves. Several morphological distinctions exist within a PV including gross coloring, free movement and disconnection with lymph nodes. The most critical difference was that the cribriform structure of PVs have multi-microsinuses, while lymph and blood capillaries are single tubular-structures and there are no sinuses inside nerve fibers. Furthermore, the histological constitution of the PV was also different from nerve fibers, blood and lymphatic capillaries. The microsinus of PVs was mainly surrounded by collagen fibers and some immune cells, and occasionally granules were observed inside sinuses. These differences have also been demonstrated in previous studies [6,27,28]. In particular, proteomic analysis of the liquid inside PVs has also been demonstrated to be distinct from that of the lymphatic liquid [29].

The sinuses of a PV were demonstrated to be flow channels in a study by Sung et al [8]. They confirmed the segregated zone in the sinuses using cryo-scanning electromicroscopy which indicated the flow of liquid [8]. Subsequently, we expected the injection dye to flow through the sinuses. In the current study, nanoparticles were observed inside a PV using TEM, as evidence of dye flow. However, they were phagocytized by immune cells just outside the sinuses in a PV, indicating that the injected nanoparticles flowing and attaching inside the sinuses could be phagocytized by adjacent immune cells in a PV in the 24-hour period between injection of dye and observation.

Several PVs entered the parenchyma of abdominal organs, such as the small intestine, urinary bladder and greater omentum. Fluorescent nanoparticles also entered the parenchyma through the PVs. This is the first report observing PVs entering the organ parenchyma. This indicates that the PV is not merely connective tissue, but a transport path of liquid to organs. If further studies are performed to investigate the entire path of PVs, and

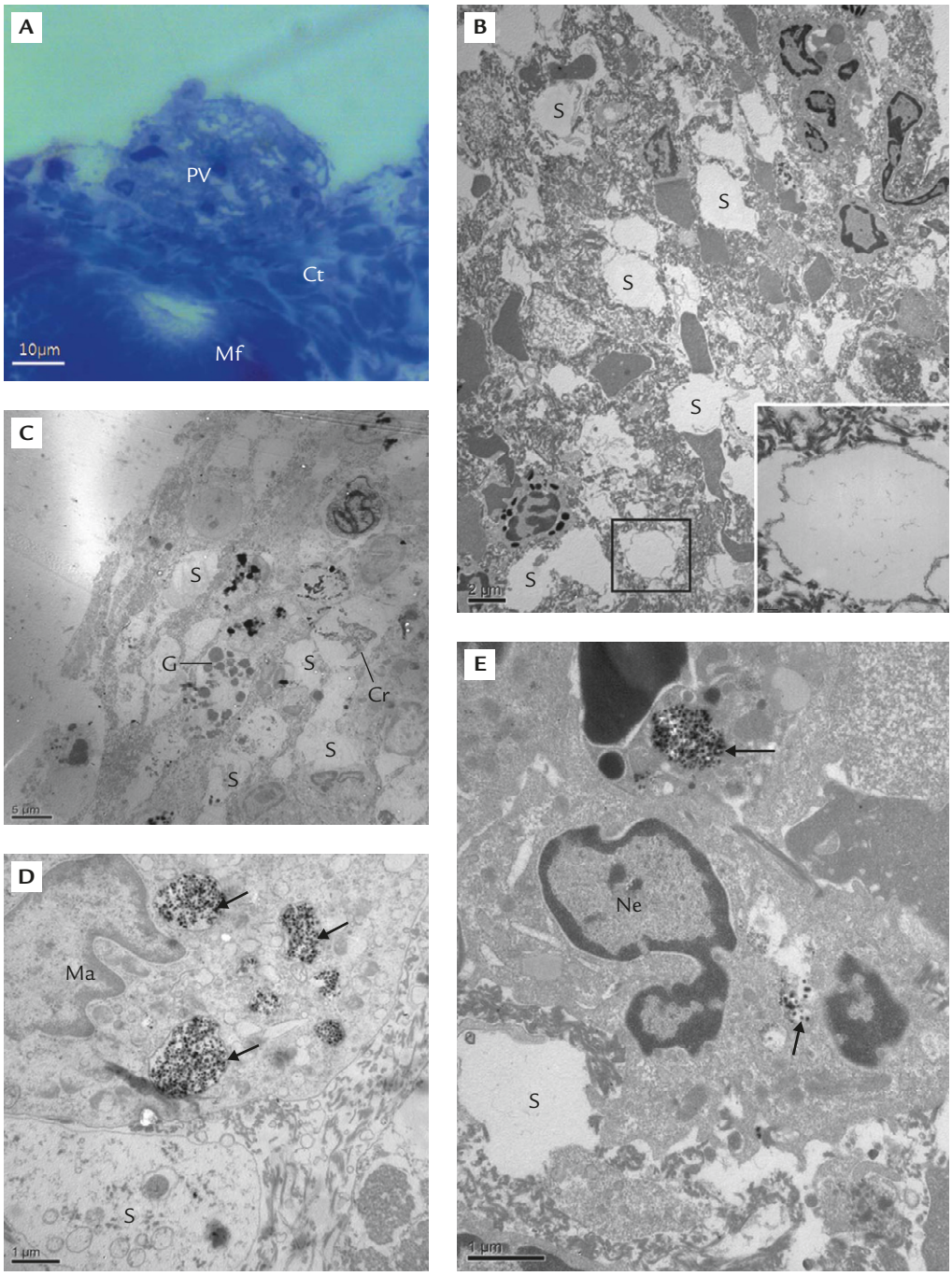

Figure 3 Photomicrographs of cross sections of the primo-vessel (PV) of a rat after injection with tracing dye. (A) A toluidine-blue-stained section showing the general morphology of the PV. (B) Electron micrograph showing numerous sinuses in the PV. A magnified image of the rectangular area shows that the boundary of the sinus is linked by a single membrane surrounded by collagenous fibers. (C) Some sinuses of the PV contain cytoplasmic granules and cellular remnants. (D) Nanoparticles (arrows) are located in the phagosomes of the macrophage just near the sinuses of the PV. (E) Nanoparticles (arrows) were engulfed by neutrophils adjacent the sinus of the PV. Ct=connective tissue; Mf=muscle fiber; S=sinus; G=cytoplasmic granules; Cr=cellular remnants; Ma=macrophages; Ne=neutrophils.

the relationship between injection points and arrival points in organs in particular, PVs could become potent drug delivery paths that exclusively transport drugs to the desired target organ without blood and lymphatic circulation.

Some immune cells and RBCs were found inside a PV or a node. The abundance of immune cells inside a PV, such as macrophages and mast cells, has been previously reported [26]. However, this is the first instance where RBCs have been observed inside

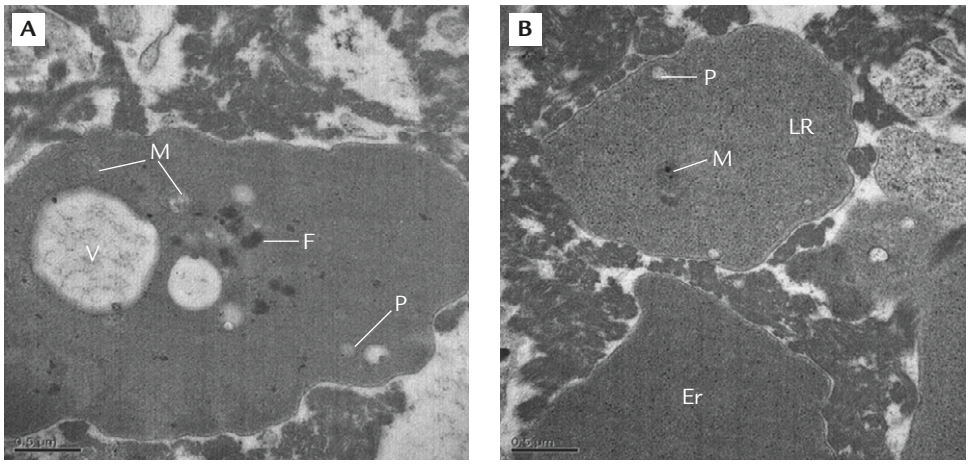

Figure 4 (A) Electron micrograph showing the presence of an early reticulocyte in the primo-vessel (PV). (B) Late reticulocyte (LR) and mature erythrocyte (Er) in the PV. These blood cells were in the extracellular matrices of collagenous fibers in the PV. P=pinocytotic vesicle; M=mitochondria; F=ferritin; V=vacuole.

a PV and a node. RBCs were observed in several nodes under a stereomicroscope, with more thorough examination with a TEM revealing immature blood cells, such as early and late reticulocytes, and mature RBCs inside the nodes and PVs. Reticulocytes are involved in hematopoiesis, are known to be mostly in bone marrow and only very few are found in the blood stream. Therefore, the presence of reticulocytes and mature RBCs in nodes and PVs is a unique and noteworthy feature. It suggests that PVs may not only be related with immune function, but also hematopoietic functions.

Several modalities have been used to visualize PVs: fluorescent nanoparticles [7,19,24] Janus Green B [17], Acridine orange staining [5,14], Feulgen reaction study [6] and Alcian blue injection [8,18]. We used Cr-Hx and fluorescent nanoparticles. Although we could not clearly define the working mechanism, we hypothesized several assumptions for its use. We selected Cr-Hx as a blue dye for easy visualization and tracing of stained structures *in vivo*. Cr-Hx is known to stain neurosecretory cells, such as hypothalamic cells [30] and since PVs contain chromaffin cells that release neurotransmitters, these cells can be well stained by Cr-Hx dye [31]. To histologically prove the flow of dye in the PVs we used fluorescent nanoparticles, which were easily detected by using both CLSM and TEM, allowing the flow in the PVs to be established histologically. Furthermore, nanoparticles are already known to flow well through PVs, thus this technique was used successfully in the current study [7,19,24].

We selected the testes as an injection point in this study as there is a large amount of reference data concerning the established flow through blood and lymphatic vessels after intratesticular injection. Therefore, intratesticular injection was considered to be an effective means for finding a novel flow structure and for comparison between a novel and established flow path. PVs were mostly detected with high reproducibility in this study. However, unfortunately, the PV network near the injection point could not be well defined. Because the dye diffused around the injection points, it was difficult to differentiate the stained structures inside the testicular parenchyma. Therefore, further studies should be conducted to better detect the PVs and to elucidate the initial network of PVs at the injection points.

In conclusion, we detected a novel flow path after intratesticular injection of Cr-Hx mixed with fluorescent nanoparticles. The path was composed of PVs, which had sinuses, collagen fibers, immune cells and hematopoietic cells. The path finally entered the parenchyma of some abdominal organs, transporting injected material to the organs. The results suggest many possibilities for the function of PV, such as involvement in immunity, hematopoiesis, and liquid flow. Therefore, further studies are needed to define the medical significance of PVs.

Acknowledgments

This work was supported in part by the Systems Biology Infrastructure Establishment Grant provided by the Gwangju Institute of Science and Technology in 2009.

References

1. McCullough DL. Experimental lymphangiography. Experience with direct medium injection into the parenchyma of the rat testis and prostate. *Invest Urol* 1975;23:211–9.
2. Head JR, Neaves WB, Billingham RE. Reconsideration of the lymphatic drainage of the rat testis. *Transplantation* 1983; 35:91–5.

3. Basal S, Irkilata HC, Yildirim I, Sadir S, Korkmaz A, Zor M, et al. Retroperitoneal lymph node mapping with intratesticular injected patent blue dye in rats. *Urol Oncol* 2008;26:286–90.
4. Russell LD, Saxena NK, Weber JE. Intratesticular injection as a method to assess the potential toxicity of various agents and to study mechanisms of normal spermatogenesis. *Gamete Res* 1987;17:43–56.
5. Lee BC, Baik KY, Johng HM, Nam TJ, Lee J, Sung B, et al. Acridine orange staining method to reveal the characteristic features of an intravascular threadlike structure. *Anat Rec* 2004;278:27–30.
6. Shin HS, Johng HM, Lee BC, Cho S, Baik KY, Yoo JS, et al. Feulgen reaction study of novel threadlike structures on the surface of rabbit livers. *Anat Rec* 2005;284:35–40.
7. Johng HM, Yoo JS, Yoon TJ, Shin HS, Lee BC, Lee C, et al. Use of magnetic nanoparticles to visualize threadlike structures inside lymphatic vessels of rats. *Evid Based Complement Alternat Med* 2007;4:77–82.
8. Sung B, Kim MS, Lee BC, Yoo JS, Lee SH, Kim YJ, et al. Measurement of flow speed in the channels of novel threadlike structures on the surfaces of mammalian organs. *Naturwissenschaften* 2008;95:117–24.
9. Soh KS. Bonghan circulatory system and acupuncture meridian. *J Acupunct Meridian Stud* 2009;2:93–106.
10. Kim BH. The Kyungrak system. *J Acad Med Sci (DPR, Korea)* 1963;90:1–41.
11. Fujiwara S, Yu SB. 'Bonghan theory': morphological studies. *Igaku no Ayumi* 1967;60:567–77.
12. Jiang X, Kim HK, Shin HS, Lee BC, Choi C, Cheun BS, et al. Method for observing intravascular Bonghan duct. *J Korean Orient Preven Med Soc* 2002;6:162–6.
13. Lee BC, Baik KY, Cho S, Min C, Johng HM, Hahm J, et al. Comparison of intravascular Bonghan ducts from rats and mice. *J Korean Orient Preven Med Soc* 2003;7:47–53.
14. Baik KY, Lee J, Lee BC, Johng HM, Nam TJ, Sung B, et al. Acupuncture meridian and intravascular Bonghan duct. *Key Eng Mater* 2005;277:125–9.
15. Lee BC, Yoo JS, Baik KY, Sung B, Lee J, Soh KS. Development of a fluorescence stereomicroscope and observation of Bong-Han corpuscles inside blood vessels. *Indian J Exp Biol* 2008:46;330–5.
16. Yoo JS, Kim MS, Ogay V, Soh KS. In vivo visualization of Bonghan ducts inside blood vessels of mice by using an Alcian blue staining method. *Indian J Exp Biol* 2008;46:336–9.
17. Lee BC, Yoo JS, Baik KY, Kim KW, Soh KS. Novel threadlike structures (Bonghan ducts) inside lymphatic vessels of rabbits visualized with a Janus Green B staining method. *Anat Rec* 2005;286:1–7.
18. Lee C, Seol SK, Lee BC, Hong YK, Je JH, Soh KS. Alcian blue staining method to visualize Bonghan threads inside large caliber lymphatic vessels and X-ray microtomography to reveal their microchannels. *Lymphat Res Biol* 2006;4:181–90.
19. Yoo JS, Johng HM, Yoon TJ, Shin HS, Lee BC, Lee C, et al. In vivo fluorescence imaging of threadlike tissues (Bonghan ducts) inside lymphatic vessels with nanoparticles. *Curr Appl Phys* 2007;4:342–8.
20. Lee BC, Soh KS. Contrast-enhancing optical method to observe a Bonghan duct floating inside a lymph vessel of a rabbit. *Lymphology* 2008;41:178–85.
21. Lee BC, Kim S, Soh KS. Novel anatomic structure in the brain and spinal cord of rabbit that may belong to the Bonghan system of potential acupuncture meridians. *J Acupunct Meridian Stud* 2008;1:29–35.
22. Cho SJ, Kim BS, Park YS. Threadlike structures in the aorta and coronary artery of swine. *J Int Soc Life Info Sci* 2004; 2:609–11.
23. Lee KJ, Kim S, Jung TE, Jin D, Kim DH, Kim HW. Unique duct system and the corpuscle-like structures found on the surface of the liver. *J Int Soc Life Info Sci* 2004;22:460–2.
24. Lee C, Yoo JS, Kim HH, Kwon J, Soh KS. Flow of nanoparticles inside organs-surface Bonghan ducts. *23th Symp Kor Soc Jungshin Sci* 2005;23:129–34. [In Korean]
25. Institute of Laboratory Animal Resources Commission on Life Sciences. *Guide for the Care and Use of Laboratory Animals*. Washington: National Academy Press, 1996.
26. Yoon TJ, Kim JS, Kim BG, Yu KN, Cho MH, Lee JK. Multifunctional nanoparticles possessing a "magnetic motor effect" for drug or gene delivery. *Angew Chem Int Ed Engl* 2005; 44:1068–71.
27. Lee BC, Yoo JS, Ogay V, Kim KW, Dobberstein H, Soh KS, et al. Electron microscopic study of novel threadlike structures on the surfaces of mammalian organs. *Microsc Res Tech* 2007;70:34–43.
28. Ogay V, Bae KH, Kim KW, Soh KS. Comparison of the characteristic features of Bonghan ducts, blood and lymphatic capillaries. *J Acupunct Meridian Stud* 2009;2:107–17.
29. Lee SJ, Lee BC, Nam CH, Lee WC, Jhang SU, Park HS, et al. Proteomic analysis for tissues and liquid from Bonghan ducts on rabbit intestinal surfaces. *J Acupunct Meridian Stud* 2008;1:1–13.
30. Fofanova KA, Postnov IuV. Neuronal secretory activity of the hypothalamic large-cell nuclei in rats with spontaneous hypertension. *Arkh Patol* 1981;43:30–5. [In Russian]
31. Kim J, Ogay V, Lee BC, Kim MS, Lim I, Woo HJ, et al. Catecholamine-producing novel endocrine organ: Bonghan system. *Med Acupunct* 2008;20:97–102.